IBRO Neuroscience Reports 13 (2022) 96–106

Contents lists available at ScienceDirect

IBRO Neuroscience Reports

journal homepage: www.sciencedirect.com/journal/IBRO-Neuroscience-Reports

Fingolimod increases parvalbumin-positive neurons in adult mice

Hiroshi Ueno [a,*], Yu Takahashi [b], Shinji Murakami [b], Kenta Wani [b], Yosuke Matsumoto [c], Motoi Okamoto [d], Takeshi Ishihara [b]

[a] Department of Medical Technology, Kawasaki University of Medical Welfare, Kurashiki 701–0193, Japan
[b] Department of Psychiatry, Kawasaki Medical School, Kurashiki 701–0192, Japan
[c] Department of Neuropsychiatry, Graduate School of Medicine, Dentistry and Pharmaceutical Sciences, Okayama University, Okayama 700–8558, Japan
[d] Department of Medical Technology, Graduate School of Health Sciences, Okayama University, Okayama 700–8558, Japan

ARTICLE INFO

Keywords:
Parvalbumin
Fingolimod
Perineuronal nets
Hippocampus
Prefrontal cortex
Somatosensory cortex

ABSTRACT

In recent years, it has been shown that central nervous system agents, such as antidepressants and antiepileptic drugs, reopen a critical period in mature animals. Fingolimod, which is used for the treatment of multiple sclerosis, also restores neuroplasticity. In this study, we investigated the effects of parvalbumin (PV)-positive neurons and perineuronal nets (PNN) on fingolimod administration with respect to neuroplasticity. Fingolimod was chronically administered intraperitoneally to mature mice. PV-positive neurons and PNN in the hippocampus, prefrontal cortex, and somatosensory cortex were analyzed. An increase in PV-positive neurons was observed in the hippocampus, prefrontal cortex, and somatosensory cortex of the fingolimod-treated mice. An increase in *Wisteria floribunda* agglutinin-positive PNN was confirmed in mice treated with fingolimod in the somatosensory cortex only. Fingolimod increased the density of PV-positive neurons in the brains of mature mice. The results indicate that fingolimod may change the critical period in mature animals.

Introduction

When the brain experiences and learns, neural networks change their structure and function according to the activity to reproduce the behavior, a property known as brain plasticity (Kolb et al., 2017). The critical period (CP) of development is characterized by enhanced neuronal plasticity (Jeanmonod et al., 1981). The critical period occurs early during postnatal development and is short-lived (Fagiolini et al., 2009). In recent years, the possibility of reopening CP has been demonstrated in mature animals (Nabel and Morishita, 2013; Begum and Sng, 2017). It has been reported earlier that central nervous system (CNS) agents, such as antidepressants and antiepileptic drugs, increase neuroplasticity (Nabel and Morishita, 2013; Begum and Sng, 2017). For example, antidepressants promote hippocampal neurogenesis (Malberg et al., 2000; Santarelli et al., 2003) and increase brain-derived neurotrophic factor (BDNF) signaling through the tropomyosin-related kinase B (TrkB) receptor (Björkholm and Monteggia, 2016; Saarelainen et al., 2003).

Fingolimod, a sphingosine-1 phosphate (S1P) receptor antagonist used for the treatment of multiple sclerosis (Brinkmann et al., 2010), has also been reported to increase BDNF (Fukumoto et al., 2014) signaling and promote neurogenesis (Efstathopoulos et al., 2015). It is a synthetic structural analog of sphingosine, which is phosphorylated by sphingosine kinase (SPHK) in vivo. Upon phosphorylation, it can activate all S1P receptors (S1PR) except S1PR2. Neurons express S1P1 and S1P3, astrocytes express S1P1 and S1P2 and oligodendrocytes express S1P1 and S1P5 (Blaho and Hla, 2014). Since fingolimod can cross the blood-brain barrier (BBB), it has potential effects on the cells of the CNS such as neurons, astrocytes, microglia, and oligodendrocytes (Blaho and Hla, 2014). Therefore, we focused on fingolimod therapy.

Fast signaling GABAergic interneurons are involved in the plasticity of the visual system during CP (Maffei et al., 2006; Yazaki-Sugiyama et al., 2009). Recent studies have shown that parvalbumin (PV) expression is a reliable surrogate for cell function and that the intensity

List of Abbreviations: CNS, central nervous system; dAC, dorsal anterior cingulate cortex; ECM, extracellular matrix; GAD67, anti-glutamic acid decarboxylase; GFAP, glial fibrillary acidic protein; IL, infralimbic cortex; NIH, National Institutes of Health, PBS, phosphate-buffered saline; PNN, perineuronal net; PL, prelimbic cortex; PV neurons, parvalbumin-expressing interneurons; WFA, *Wisteria floribunda* agglutinin.

* Correspondence to: Department of Medical Technology, Kawasaki University of Medical Welfare, 288 Matsushima, Kurashiki, Okayama 701–0193, Japan, 193.
E-mail addresses: dhe422007@s.okayama-u.ac.jp (H. Ueno), yuuu.takahashi@gmail.com (Y. Takahashi), muraka@med.kawasaki-m.ac.jp (S. Murakami), k-wani@med.kawasaki-m.ac.jp (K. Wani), ymatsumoto@cc.okayama-u.ac.jp (Y. Matsumoto), mokamoto@md.okayama-u.ac.jp (M. Okamoto), t-ishihara@med.kawasaki-m.ac.jp (T. Ishihara).

https://doi.org/10.1016/j.ibneur.2022.06.005
Received 25 January 2022; Received in revised form 28 June 2022; Accepted 29 June 2022
Available online 1 July 2022

of cortical PV staining is correlated with an experience-dependent degree of plasticity (Rowlands et al., 2018; Donato et al., 2013). In addition, perineuronal nets (PNN) are extracellular matrix containing structures that regulate plasticity. They preferentially deposit around PV-positive neurons in an activity-dependent manner (Dityatev et al., 2007; Favuzzi et al., 2017).

PV is a calcium-buffering protein that regulates synaptic plasticity over a short period of time (Caillard et al., 2000). Perisomatic inhibition by PV-positive neurons regulates pyramidal neuron spikes and network oscillations through feedforward and feedback inhibition (Sun et al., 2014; Sohal et al., 2009). Importantly, changes in the PV network configuration interfere with experience-dependent plasticity mechanisms in the brain and are associated with motor learning deficiencies (Donato et al., 2013). It has been suggested that fast spike-mediated neurons are involved in the development of cortical ocular dominance and ocular dominance plasticity in juvenile mice (Smith and Bear, 2010; Yazaki-Sugiyama et al., 2009).

The extracellular matrix (ECM) in the CNS is composed of hyaluronic acid, tenescin-R, glycoprotein, and chondroitin sulfate proteoglycan (Maeda, 2015). In the mature CNS, ECM molecules are disseminated as nerve granules or as PNN, which is a concentrated reticulated structure (Maeda, 2015). PNN form a network-like structure that covers the cell body, axon initial segment, and proximal dendrite of a specific neuron in the CNS (Slaker et al., 2016). Multiple PNN form around PV-positive neurons, which are GABAergic interneurons (Carulli et al., 2010; Deepa et al., 2006).

The purpose of this study was to investigate the effect of chronic fingolimod administration on the formation of PV-positive neurons and PNN involved in neuroplasticity. In this study, we focused on the hippocampus, somatosensory cortex, and prefrontal cortex of mice. The findings of our study may provide an opportunity to develop therapeutic approaches for the recovery of brain plasticity post-maturity.

Materials and Methods

Animals

Eleven week old male mice (C57BL/6 N) were purchased from Charles River Laboratories (Kanagawa, Japan). Five mice were housed in each cage under standard laboratory conditions. All procedures related to animal maintenance and study designs were approved by the Committee for Animal Experiments at Kawasaki Medical School Advanced Research Center and conformed to the U.S. National Institutes of Health (NIH) Guide for the Care and Use of Laboratory Animals (NIH Publication No. 80–23, revised in 1996). The mice were provided food and water ad libitum and were kept under the following conditions: lights on at 7:00 A.M., lights off at 9:00 P.M., and temperature maintained at 23–26 °C.

Drug protocol

All the mice were randomized into two groups (n = 10). Fingolimod (067–06253, FUJIFILM Wako, Tokyo, Japan) was dissolved in saline to obtain a final concentration of 3 mg/mL. The mice were injected intraperitoneally (i.p.) with 6 mg/kg fingolimod for 35 days. The dose of fingolimod was determined from previously reported doses (di Nuzzo et al., 2015). The vehicle control mice were injected with saline. On day 35, the mice were sacrificed and their brains were extracted for further analysis.

Tissue preparation

The mice were anesthetized with a lethal dose of sodium pentobarbital (120 mg/kg, i.p.) and transcardially perfused with 25 mL of phosphate-buffered saline (PBS), followed by 100 mL of 4% paraformaldehyde in PBS (pH 7.4). The brains were dissected and fixed overnight at 4 °C in a fixative, cryopreserved in 15% sucrose for 12 h, followed by preservation in 30% sucrose for 20 h at 4 °C. Next, the brains were frozen in an optimum cutting temperature compound (Tissue-Tek; Sakura Finetek, Tokyo, Japan) using a slurry of normal hexane in dry ice. Serial coronal sections with a thickness of 40 μm were obtained at − 20 °C using a cryostat (CM3050S; Leica Wetzlar, Germany). The sections were collected in ice-cold PBS containing 0.05% sodium azide.

Immunohistochemistry

The sections were treated with 0.1% Triton X-100 and PBS at room temperature for 15 min. After three washes with PBS, sections were incubated with 10% normal goat serum (ImmunoBioScience Corp., Mukilteo, WA, USA) in PBS at room temperature for 1 h. They were then washed thrice with PBS and incubated overnight at 4 °C in PBS containing biotinylated *Wisteria floribunda* agglutinin (WFA) (B-1355, Vector Laboratories; 1:200) and/or antibodies described in the subsequent text. After washing with PBS, the sections were incubated with Alexa Fluor 594-conjugated streptavidin (S11227; Molecular Probes, Eugene, OR) and/or the corresponding secondary antibodies (described in the subsection Antibodies and lectins) at room temperature for 2 h. The labeled sections were then rinsed with PBS and mounted on glass slides using Vectashield medium (H-1400; Vector Laboratories, Funakoshi Co., Tokyo, Japan). The prepared slides were stored at 4 °C until microscopic analysis was performed.

Lectins and antibodies

The following lectins and primary antibodies were used for staining: biotinylated WFA (B-1355, Vector Laboratories; 1:200), mouse anti-parvalbumin (clone PARV-19, P3088; Sigma-Aldrich Japan, Tokyo, Japan; 1:1000), mouse anti-aggrecan (Cat-315; MAB1581, MERCK; 1:1000), rabbit anti-aggrecan (AB1031, Millipore, Tokyo, Japan; 1:200), rabbit anti-glial fibrillary acidic protein (GFAP) (ab7260; Abcam, Cambridge, MA; 1:1000), rabbit anti-ionized calcium-binding adapter molecule 1 (Iba-1) (019–19741; FUJIFILM Wako Pure Chemical Corporation, Osaka, Japan; 1:1000), mouse anti-NeuN (clone A60, MAB377; Millipore; 1:500), and mouse anti-glutamate decarboxylase (GAD67) (clone 1G10.2, MAB5406; Millipore, Bedford, MA; 1:1000).

The following secondary antibodies were used for visualization: Alexa Fluor 488-conjugated goat anti-mouse IgG (ab150113; Abcam, Cambridge, MA; 1:1000), FITC-conjugated anti-mouse IgM (sc-2082, Santa Cruz Biotechnology, Santa Cruz, CA, 1:1000), Texas Red-conjugated goat anti-rabbit (TI-1000; Vector Laboratories, Funakoshi Co., Tokyo, Japan), and streptavidin-conjugated Alexa Fluor 594 (S11227, Thermo Fisher Scientific; 1:1000).

Microscopy imaging

To quantify the density of PV, WFA, Cat-315, AB1031, and GFAP-positive cells, confocal laser scanning microscopy (LSM700; Carl Zeiss, Oberkochen, Germany) was used. Images (1024 × 1024 pixels) were saved as TIFF files using ZEN software (Carl Zeiss). Briefly, a 10 × numerical aperture (NA = 0.45) or 20 × (NA = 0.8) objective lens and pinhole setting that corresponded to a focal plane thickness of less than 1 μm was used. PV, WFA, Cat-315, AB1031, and GFAP-positive cells were counted in a 1.0 × 1.2 mm area spanning all layers of the cortex. Prior to capture, the exposure time, gain, and offset were carefully set to ensure a strong signal but avoid saturation. Identical capture conditions were used for all the sections.

Quantification of labeled cells and PNNs

The brain regions were determined according to the mouse brain atlas of Paxinos and Franklin (2013). The data shown in the figures are

presented according to the cortical layer profiles based on fluorescence Nissl staining (NeuroTrace 435/455 blue: N-21479, Molecular Probes, Thermo Fisher Scientific, U.S.). Microphotoimages of the sections were taken with a 10 × or 20 × objective. All confocal images were saved as TIFF files and analyzed using the NIH ImageJ software (Bethesda, MD; http://rsb.info.nih.gov/nih-image/). Twelve coronal sections containing the dorsal hippocampus (−1.58 to −2.06 mm relative to the bregma), prefrontal (2.22 – 1.70 mm relative to the bregma), and somatosensory cortices (−0.94 to −1.58 mm relative to the bregma) were selected from each mouse and stained. The stained neurons and PNN (neuronal soma size > 60 μm^2) in the region of interest were manually tagged and counted. The background intensity was subtracted from the unstained portions of each section. The density of the labeled neurons was calculated as cells/mm^2. Quantification was performed by an independent observer blinded to the identity of the specimens.

Data analysis

Data were expressed as box plots of 10 animals per group. Statistical analyses were performed using SPSS Statistics software (IBM Corp., Armonk, NY, USA). Student's t-test was performed for single comparisons and analysis of variance (ANOVA) for multiple comparisons (two-way ANOVA followed by Bonferroni t-tests). Bonferroni post-hoc comparisons were conducted when the interaction terms were significant. Statistical significance was set at $p < 0.05$.

Results

PV-positive neurons and WFA-positive PNN in the hippocampus, prefrontal cortex, and somatosensory cortex of fingolimod-treated mice

To analyze the effect of chronic fingolimod administration on the distribution of PV-positive neurons, coronal sections were immunostained for PV proteins (Fig. 1A, A′, C, C′, E, E′). To examine the spatial distribution of PNN, we performed immunostaining with WFA (Fig. 1B, B′, D, D, F′, F′). The distribution of PV-positive neurons and WFA-positive PNN in the hippocampal prefrontal cortex and somatosensory cortex of fingolimod-treated mice was similar to that observed in the control mice.

We quantified PV-positive neurons and WFA-positive PNN in the hippocampus, prefrontal cortex, and somatosensory cortex of fingolimod-treated mice (Figs. 2–4).

The effect of fingolimod administration on PV-positive neurons and WFA-positive PNN in the hippocampus

In the CA1 and DG regions of the hippocampus, the density of PV-positive neurons was higher in the fingolimod-treated mice than in the control mice (Fig. 2A; $F_{2,36} = 8.031$, $p = 0.005$, CA1: $p = 0.001$, CA3: $p = 0.992$, and DG: $p = 0.045$). In the CA3 area, there was no difference in the density of PV-positive neurons between the fingolimod-treated and the control mice. No difference was observed in the density of WFA-positive PNN for the hippocampi of the fingolimod-treated and the control mice (Fig. 2B; $F_{2,36} = 0.584$, $p = 0.446$). There was also no significant difference between the percentage of PV-positive neurons surrounded by WFA-positive PNN in the hippocampi of the fingolimod-treated and the control mice (Fig. 2 C; $F_{2,36} = 0.424$, $p = 0.516$). Additionally, in the CA1 and DG regions of the hippocampus, the percentage of WFA-positive PNN containing PV was higher in the fingolimod-treated mice than in the control mice (Fig. 2D; $F_{2,36} = 6.176$, $p = 0.015$, CA1: $p = 0.074$, CA3: $p = 0.354$, and DG: $p = 0.002$).

The effect of fingolimod administration on PV-positive neurons and WFA-positive PNN in the prefrontal cortex

In the L5/6 cortical layer of the dorsal anterior cingulate cortex (dAC), L5/6 layer of the prelimbic cortex (PL), and L2/3 and L5/6 layers of the infralimbic cortex (IL), the density of PV-positive neurons was higher in the fingolimod-treated mice than in the control mice (Fig. 3A; dAC, $F_{1,18} = 10.190$, $p = 0.002$, L2/3: $p = 0.492$, and L5/6: $p < 0.001$, PL, $F_{1,18} = 7.606$, $p = 0.008$, L2/3: $p = 0.252$, and L5/6: $p = 0.009$, IL, $F_{1,18} = 13.037$, $p < 0.001$, L2/3: $p = 0.001$, and L5/6: $p = 0.002$). However, there was no difference in the density of WFA-positive PNN between the fingolimod-treated and the control mice for the dAC, PL, and IL groups (Fig. 3B; dAC, $F_{1,18} = 8.461$, $p = 0.005$, L2/3: $p = 0.772$, and L5/6: $p = 0.122$, PL, $F_{1,18} = 5.974$, $p = 0.017$, L2/3: $p = 0.068$, and L5/6: $p = 0.121$, IL, $F_{1,18} = 0.677$, $p = 0.414$). There were no significant difference in the percentage of PV-positive neurons surrounded by WFA-positive PNN in the dAC and PL of the fingolimod-treated and the

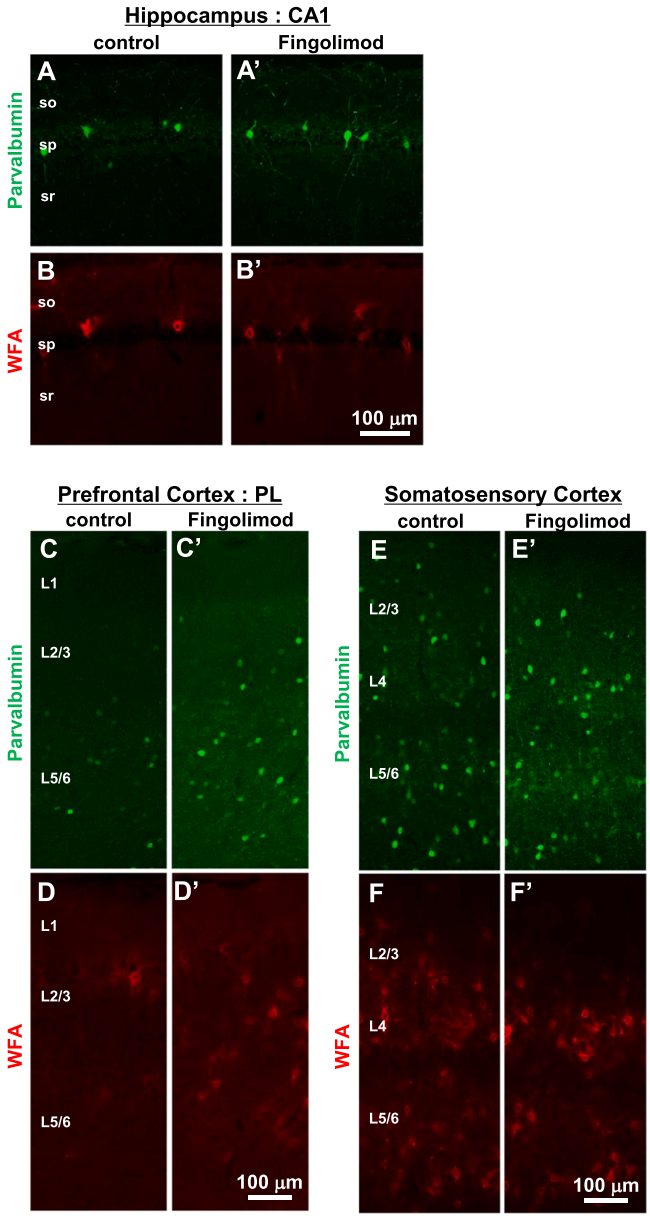

Fig. 1. Distribution of PV-positive neurons and WFA-positive PNN in the hippocampus, prefrontal cortex, and somatosensory cortex of fingolimod-treated mice, Representative double immunofluorescence images show the distribution of PV-positive neurons (A, A′, C, C′, D, D′) and WFA-positive PNNs (B, B′, D, D′, F, F′) in the CA1 of the hippocampus (A, A′, B, B′), PL of the prefrontal cortex (C, C′, D, D′), and somatosensory cortex (E, E′, F, F′) of control (A-F) and fingolimod-treated mice (A′-F′). Scale bar = 100 μm in B′ (A, A′, B, B′), 100 μm in D′ (C, C′, D, D′), and 100 μm in F′ (E, E′, F, F′).

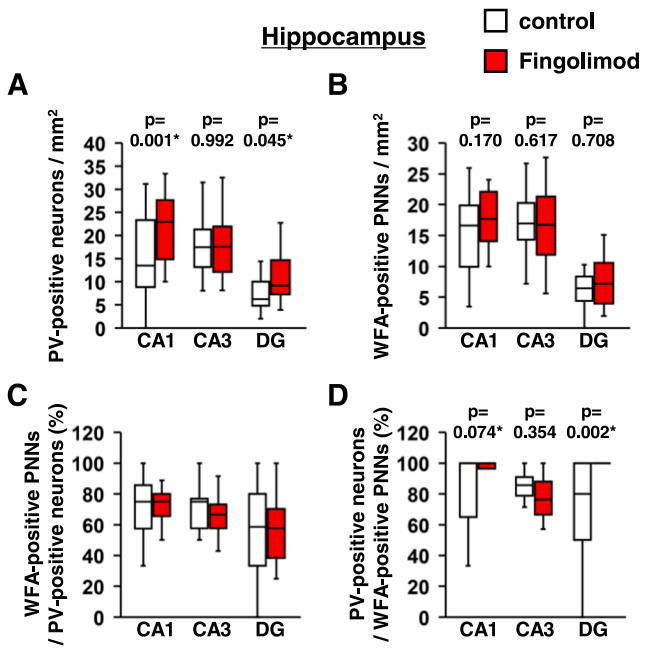

Fig. 2. Quantitative analyses of PV-positive neurons and WFA-positive PNNs in the fingolimod-treated mouse hippocampus, Region-specific patterns of PV-positive neuron density (A) and WFA-positive PNN density (B) in the hippocampus. The percentage of PV-positive neurons surrounded by WFA-positive PNN (C) and the percentage of WFA-positive PNNs containing PVs (D) in the hippocampus are shown. Data are expressed as box plots (n = 10 mice/group). P-values were calculated using two-way ANOVA. *p < 0.05 for comparison of the same regions between fingolimod-treated groups.

control mice (Fig. 3**C**; dAC, $F_{1,18} = 0.540$, $p = 0.465$, PL, $F_{1,18} = 0.012$, $p = 0.913$, IL, $F_{1,18} = 7.071$, $p = 0.011$, L2/3: $p = 0.031$, and L5/6: $p = 0.039$). In L2/3 layer of IL, the percentage of PV-positive neurons surrounded by WFA-positive PNN was higher in the fingolimod-treated mice than in the control mice. In L5/6 layer of IL, the percentage of PV-positive neurons surrounded by WFA-positive PNN was lower in the fingolimod-treated mice than in the control mice. There was no significant difference between the percentage of WFA-positive PNN containing PV in the dAC, PL, and IL of the fingolimod-treated and the control mice (Fig. 3**D**; dAC, $F_{1,18} = 0.945$, $p = 0.335$, PL, $F_{1,18} = 0.422$, $p = 0.518$, IL, $F_{1,18} = 0.165$, $p = 0.686$).

The effect of fingolimod administration on PV-positive neurons and WFA-positive PNN in the somatosensory cortex

In L4 and L5/6 of the somatosensory cortex, the density of PV-positive neurons was higher in the fingolimod-treated mice than in the control mice (Fig. 4A; $F_{2,36} = 11.421$, $p < 0.001$, L2/3: $p = 0.921$, L4: $p = 0.003$, and L5/6: $p < 0.001$). In L4 and L5/6 of the somatosensory cortex, the density of WFA-positive PNNs was higher in the fingolimod-treated mice than in the control mice (Fig. 4B; $F_{2,36} = 19.079$, $p < 0.001$, L2/3: $p = 0.904$, L4: $p < 0.001$, and L5/6: $p = 0.042$). There was no significant difference in the percentages of PV-positive neurons surrounded by WFA-positive PNN in the somatosensory cortex of the fingolimod-treated and the control mice (Fig. 4C; $F_{2,36} = 0.552$, $p = 0.459$). In addition, there was no significant difference in the percentage of WFA-positive PNN containing PV in the somatosensory cortex of the control and the fingolimod-treated mice (Fig. 4D; $F_{2,36} = 0.049$, $p = 0.826$, L2/3: $p = 0.338$, L4: $p = 0.754$, and L5/6: $p = 0.745$).

GAD67-positive neurons in the hippocampus, prefrontal cortex, and somatosensory cortex of Fingolimod-treated mice

We examined the distribution of GAD67-positive neurons in the hippocampus, prefrontal cortex, and somatosensory cortex of the fingolimod-treated mice (Fig. 5A). The distribution of GAD67-positive neurons in the hippocampus, prefrontal cortex, and somatosensory cortex of the fingolimod-treated mice was similar to that observed in the control mice.

We quantified GAD67-positive neurons in the hippocampus, prefrontal cortex, and somatosensory cortex of the fingolimod-treated mice (Figs. 6–8).

The density of GAD67-positive neurons in the CA3 region of the hippocampus was higher in the fingolimod-treated mice than in the control mice (Fig. 6A; $F_{2,36} = 6.692$, $p = 0.011$, CA1: $p = 0.228$, CA3: $p = 0.039$, and DG: $p = 0.135$). In other areas, there was no difference in the density of GAD67-positive neurons between the fingolimod-treated and the control mice (Fig. 7A; dAC, $F_{2,36} = 0.008$, $p = 0.927$, PL, $F_{2102} = 0.269$, $p = 0.605$, IL, $F_{2,36} = 0.057$, $p = 0.811$, **and 8 A**; $F_{3,54} = 1.365$, $p = 0.245$).

The percentage of GAD67-positive neurons containing PV in the L5/6 layer of the prefrontal cortex was higher in the fingolimod-treated mice than in the control mice (Fig. 7**B**). In other areas, there was no difference in the percentage of GAD67-positive neurons containing PV between the fingolimod-treated and the control mice (Fig. 6**B**; $F_{2,36} = 3.664$, $p = 0.058$, **7B**; dAC, $F_{2,36} = 3.483$, $p = 0.065$, PL, $F_{2,36} = 6.704$, $p = 0.010$, L2/3: $p = 0.092$, and L5/6: $p = 0.129$, IL, $F_{2,36} = 3.182$, $p = 0.078$, L2/3: $p = 0.940$, and L5/6: $p = 0.016$**, and 8B**; $F_{3,54} = 2.131$, $p = 0.147$).

PNN components in the hippocampus and somatosensory cortex of Fingolimod-treated mice

To examine the composition of PNN in the hippocampus and somatosensory cortices in the fingolimod-treated mice, we labeled PNN with WFA lectin as well as AB1031 and Cat-315 anti-aggrecan antibodies (Fig. 9). The distribution of Cat-315-positive PNNs and AB1031-positive PNNs in the hippocampus and somatosensory cortex of the fingolimod-treated mice was similar to that observed in the control mice.

We quantified Cat-315-positive PNN and AB1031-positive PNN in the hippocampus and somatosensory cortex of the fingolimod-treated mice (Figs. 10–11). There was no significant difference in the density of Cat-315-positive PNN in the hippocampi of the fingolimod-treated and the control mice (Fig. 10A; $F_{2,36} = 1.048$, $p = 0.311$). There was no significant difference in the density of AB1031-positive PNN and Cat-315-positive PNN containing AB1031 in the hippocampi of the fingolimod-treated and the control mice (Fig. 10B; $F_{2,36} = 0.431$, $p = 0.515$, C; $F_{2,36} = 0.340$, $p = 0.563$). The percentage of AB1031-positive PNN containing Cat-315 in the DG of the hippocampus was higher in the fingolimod-treated mice than in the control mice (Fig. 10D; $F_{2,36} = 4.760$, $p = 0.034$, CA3: $p = 0.702$, and DG: $p = 0.001$).

There was no difference in the density of Cat-315 and AB1031-positive PNN in the somatosensory cortex for the fingolimod-treated and the control mice (Fig. 11A; $F_{2,36} = 2.276$, $p = 0.138$, **B**; $F_{2,36} = 1.794$, $p = 0.187$). In L2/3 layer of the somatosensory cortex, the percentage of Cat-315-positive PNN containing AB1031 was lower in the fingolimod-treated mice than in the control mice (Fig. 11C; $F_{2,36} = 17.285$, $p < 0.001$, L2/3: $p < 0.001$, L4: $p = 0.170$, and L5/6: $p = 0.402$). There was no difference in the percentage of AB1031-positive PNN containing Cat-315 in the somatosensory cortex for the fingolimod-treated and the control mice (Fig. 11D; $F_{2,36} = 3.879$, $p = 0.055$).

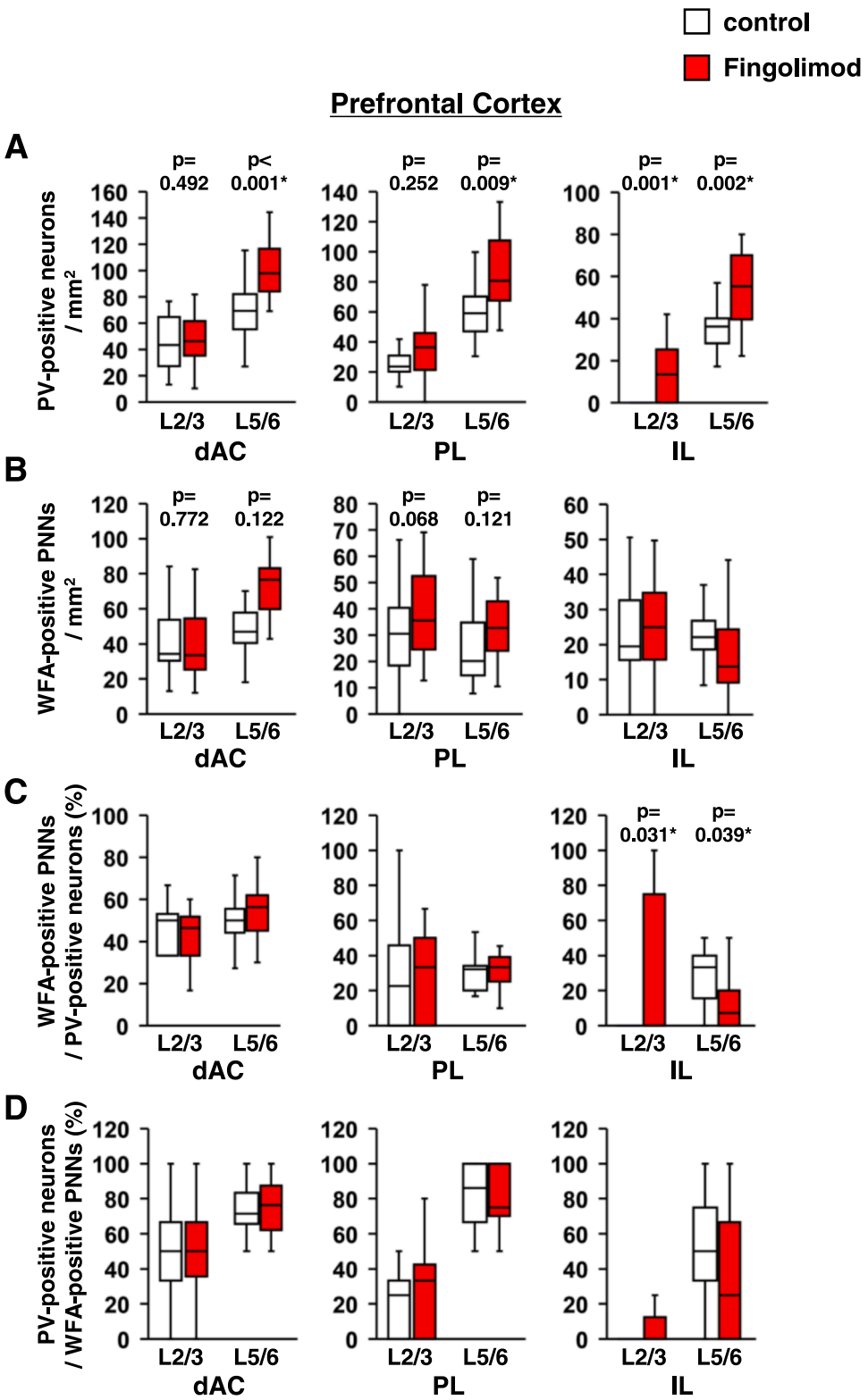

Fig. 3. Quantitative analyses of PV-positive neurons and WFA-positive PNNs in the fingolimod-treated mouse prefrontal cortex, Layer-specific patterns of PV-positive neuron density (A) and WFA-positive PNN density (B) in the PFC are shown. The percentage of PV-positive neurons surrounded by WFA-positive PNN (C) and the percentage of WFA-positive PNN containing PVs (D) in the prefrontal cortex are shown. Data are expressed as box plots (n = 10 mice/group). P-values were calculated using two-way ANOVA. *p < 0.05 for comparison of the same layers between the fingolimod-treated groups.

GFAP-positive astrocytes, NeuN-positive cells, and Iba-1-positive microglia in the hippocampus of fingolimod-treated mice

To analyze the effect of chronic fingolimod administration on the activation of astrocytes, the coronal sections were immunostained for GFAP proteins (Fig. 12A, B). There were no significant difference between the fingolimod-treated and the control mice with respect to the areas containing GFAP-positive astrocytes in the CA1 region of the hippocampus (Fig. 12C; $t = -1.722$, $p = 0.080$).

The distribution of NeuN-positive cells in the CA1 region of the hippocampus of the fingolimod-treated mice was also examined (Fig. 12D, E). The fingolimod-treated mice showed no changes in the distribution of NeuN-positive cells in the hippocampus as compared to the control mice.

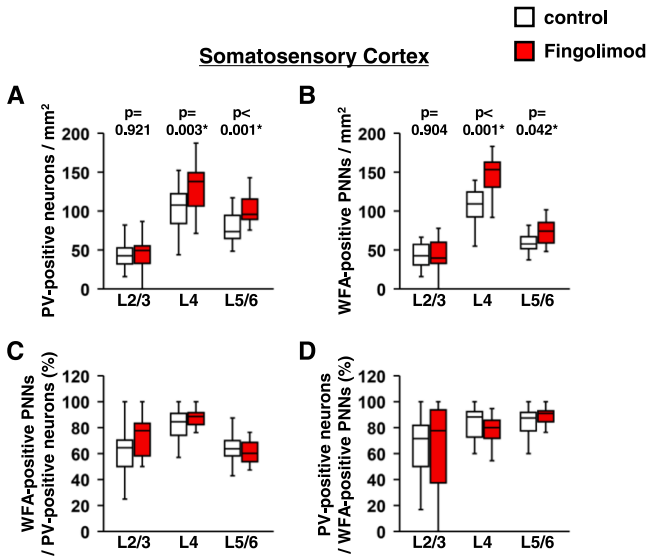

Fig. 4. Quantitative analyses of PV-positive neurons and WFA-positive PNNs in the Fingolimod-treated mouse somatosensory cortex, Layer-specific patterns of PV-positive neuron density (A) and WFA-positive PNN density (B) in the somatosensory cortex. The percentage of PV-positive neurons surrounded by WFA-positive PNNs (C) and the percentage of WFA-positive PNNs containing PVs (D) in the somatosensory cortex are shown. Data are expressed as box plots ($n = 10$ mice/group). P-values were calculated using two-way ANOVA. *$p < 0.05$ for comparison of the same layers between the fingolimod-treated groups.

To assess whether fingolimod administration affected immune activation in the cerebral cortex of mice, the morphology of Iba-1-positive microglia in the CA1 of the hippocampus was examined (Fig. 12F-G). Iba-1-positive microglia were found in the CA1 region of the hippocampus in the fingolimod-treated mice. There were no significant morphological differences in Iba-1-positive microglia for the fingolimod-treated and the control mice.

To analyze the effect of fingolimod administration on neurogenesis in the DG, we observed the GFAP-immunostained DG of the hippocampus (Fig. 12H, I). Fingolimod-treated mice showed no apparent changes in the distribution of GFAP-positive cells in the DG of the hippocampus as compared to the control mice.

Discussion

The results of this study showed that chronic administration of fingolimod increased the density of PV-positive neurons in the prefrontal cortex, somatosensory cortex, and hippocampus. The fingolimod-treated mice showed an increase in the number of WFA-positive PNN in the somatosensory cortex as compared to the control mice.

To the best of our knowledge, there are no reports on the compounds that increase parvalbumin-positive neurons. In the PV-positive neurons of the sensory cortex, the expression level of PV proteins depends on the input stimulus (Caballero et al., 2013). Therefore, the number of PV neurons increases with brain development throughout and then becomes constant (Schmalbach et al., 2015; Ueno et al., 2017, 2017b, 2018). Further, it is also known that fingolimod (FTY720) increases BDNF expression (Deogracias et al., 2012; Vidal-Martínez et al., 2016). BDNF is a neurotrophin that is secreted by the basal forebrain cholinergic neurons and is involved in the synaptic plasticity required for long-term memory (Tyler et al., 2002). It has been reported to increase PV protein expression (Huang et al., 1999), which may explain the increase in PV-positive neurons in this study. Alternatively, it is possible that the PV expression density of each neuron remains the same and the number of PV neuron nuclei increases. Further research is needed to find

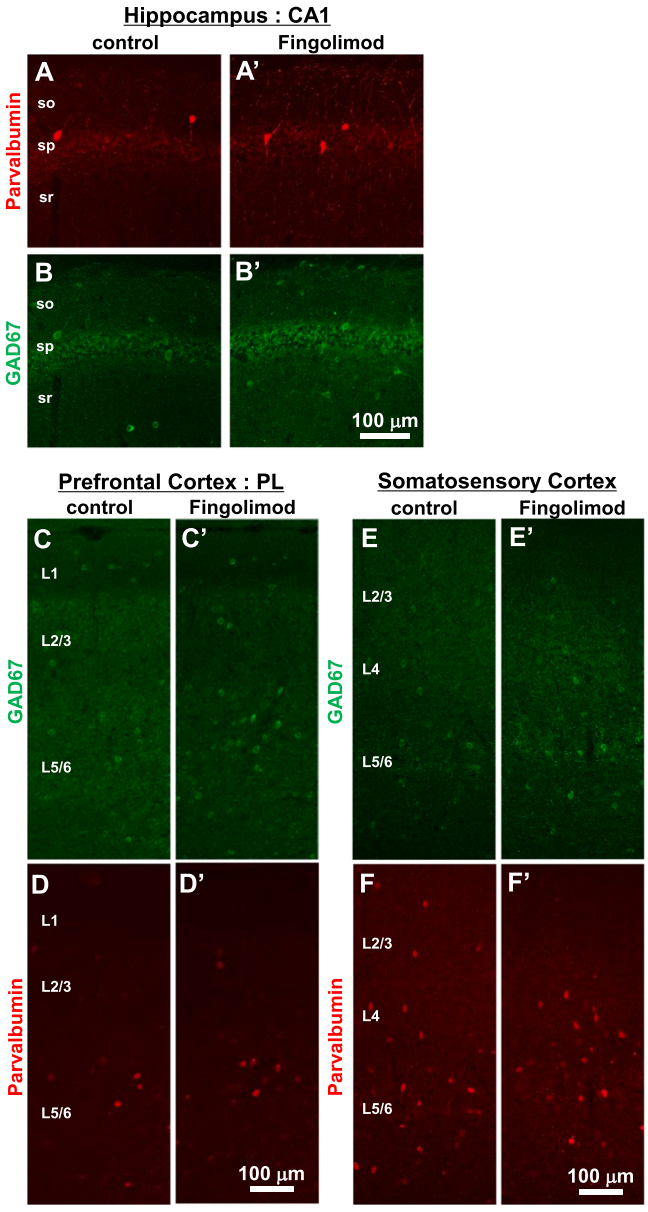

Fig. 5. Distribution of PV-positive neurons and GAD67-positive neurons in the hippocampus, prefrontal cortex, and somatosensory cortex of fingolimod-treated mice, Representative double immunofluorescence images show the distribution of PV-positive neurons (A, A′, C, C′, D, D′) and GAD67-positive neurons (B, B′, D, D′, F, F′) in the CA1 of the hippocampus (A, A′, B, B′), PL of the prefrontal cortex (C, C′, D, D′), and somatosensory cortex (E, E′, F, F′) of control (A-F) and fingolimod-treated mice (A′-F′). Scale bar = 100 μm in B′ (A, A′, B, B′), 100 μm in D′ (C, C′, D, D′), and 100 μm in F′ (E, E′, F, F′).

out more.

We observed an increase in the WFA-positive PNN of the somatosensory cortex of the fingolimod-treated mice. However, there was no significant difference in the proportion of PV-positive neurons covered with WFA-positive PNN, suggesting that an increase in WFA-positive PNN was associated with an increase in PV-positive neurons. WFA-positive PNN are present throughout the brain in the mature rodent cortex (Alpár et al., 2006; Horii-Hayashi et al., 2015; Brückner et al., 2000, 2003). WFA-positive PNNs differ in their density, the expression levels of WFA-positive molecules, the mesh-like structure of PNNs, and the ratio of WFA-positive PNNs covering PV-positive neurons depending on the brain region (Horii-Hayashi et al., 2015; Ueno et al., 2017b, 2018). There are also highly plastic areas in the mature brain cortex,

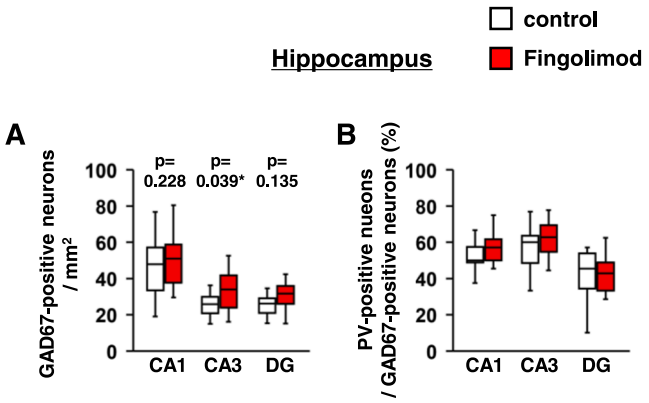

Fig. 6. Quantitative analyses of GAD67-positive neurons in the hippocampus of fingolimod-treated mice, Region-specific patterns of GAD67-positive neuron density (A) and percentage of GAD67-positive neurons containing PV (B) in the hippocampus are shown. Data are expressed as box plots (n = 10 mice/group). P-values were calculated using two-way ANOVA. *p < 0.05 for comparison of the same regions between fingolimod-treated groups.

such as the frontal and associative cortices, which remain highly plastic throughout the lifespan (Kolb and Gibb, 2015; Jung et al., 2008; Chapman et al., 2008; Canto et al., 2008; Sadato et al., 2004). WFA-positive PNNs are present in all the cortices. Further studies are needed to investigate changes in WFA-positive PNNs in unexamined brain regions of fingolimod-treated mice. Nonetheless, our results indicate that fingolimod is not involved in plasticity by altering WFA-positive PNNs in the somatosensory cortex.

It has been previously reported that expression of aggrecan in PNN is sensory input-dependent and regulates the completion of the critical period (Sur, 1988; Hockfield and Sur, 1990). Many reports have shown that aggrecan, a component of PNN, may be involved in plasticity (McRae et al., 2007; Ueno et al., 2017; Nakamura et al., 2009; Ye and Miao, 2013). Cat-315 recognizes a subset of the HNK-1 (human natural killer-1) epitope on aggrecan (Dino et al., 2006) and has been reported to be associated with synaptic plasticity (Senn et al., 2002). A decrease in Cat-315-positive PNN suggests an increase in synaptic plasticity. In this study, there was almost no change in the number of Cat-315-positive PNN or AB1031-positive PNN.

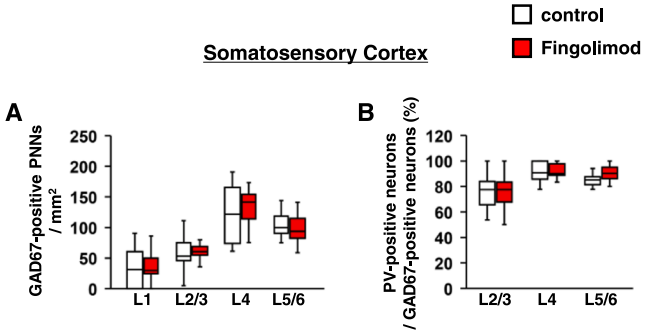

Fig. 8. Quantitative analyses of GAD67-positive neurons in the somatosensory cortex of fingolimod-treated mice, Layer-specific patterns of GAD67-positive neuron density (A) and the percentage of GAD67-positive neurons containing PV (B) in the somatosensory cortex are shown. Data are expressed as box plots (n = 10 mice/group). P-values were calculated using two-way ANOVA. *p < 0.05 for comparison of the same regions between fingolimod-treated groups.

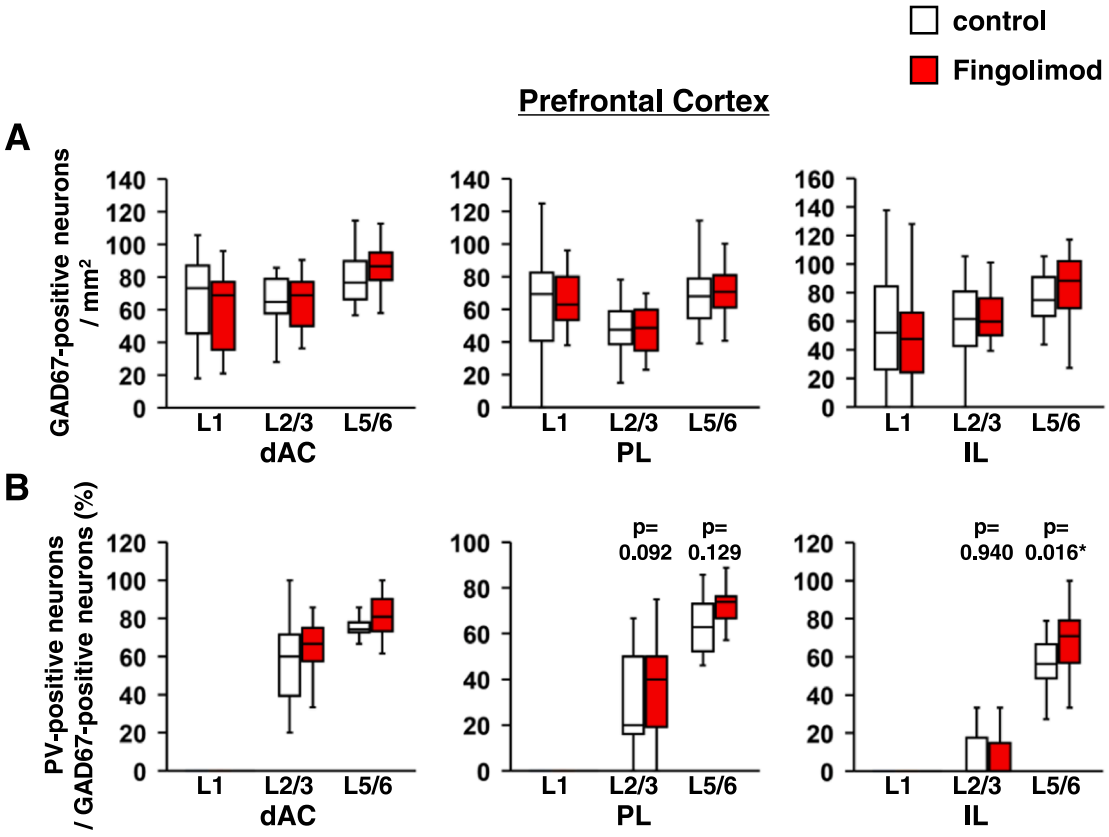

Fig. 7. Quantitative analyses of GAD67-positive neurons in the prefrontal cortex of fingolimod-treated mice, Layer-specific patterns of GAD67-positive neuron density (A) and percentage of GAD67-positive neurons containing PV (B) in the prefrontal cortex are shown. Data are expressed as box plots (n = 10 mice/group). P-values were calculated using two-way ANOVA. *p < 0.05 for comparison of the same regions between fingolimod-treated groups.

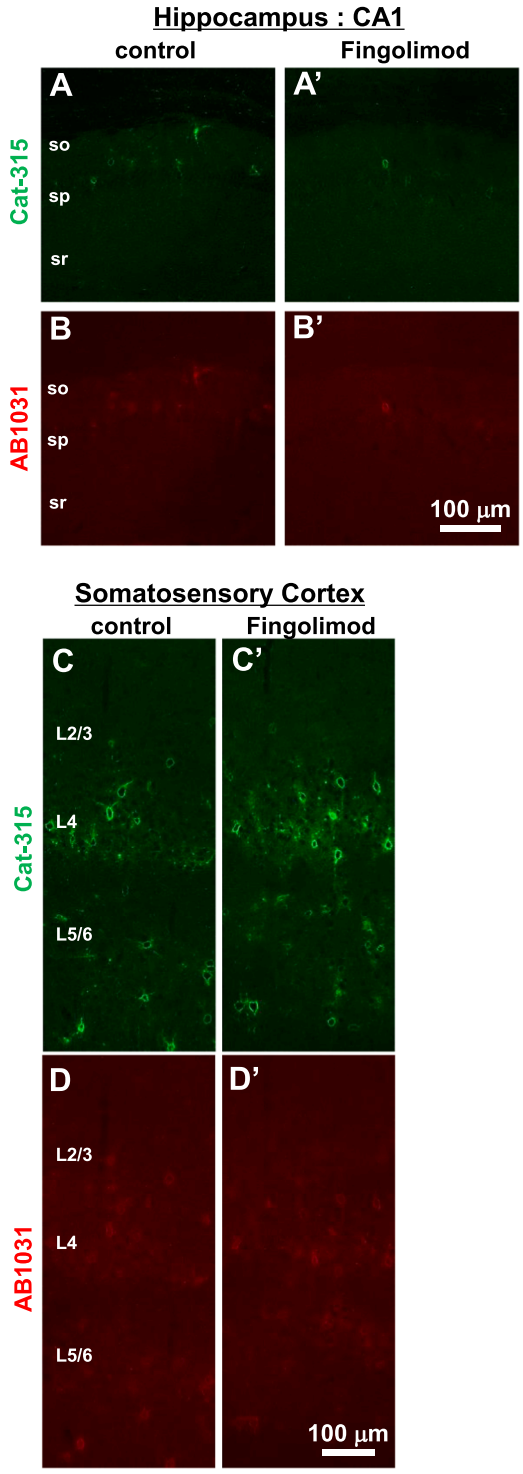

Fig. 9. Distribution of Cat-315-positive PNNs and AB1031-positive PNNs in the hippocampus and somatosensory cortex of fingolimod-treated mice, Representative double immunofluorescence images show the distribution of Cat-315-positive PNNs (A, A′, C, C′) and AB1031-positive PNSs (B, B′, D, D′) in the CA1 of the hippocampus (A, A′, B, B′) and somatosensory cortex (C, C′, D, D′) of control (A-D) and fingolimod-treated mice (A′-D′). Scale bar = 100 μm in B′ (applied to A, A′, B, B′) and 100 μm in D′ (applied to C, C′, D, D′).

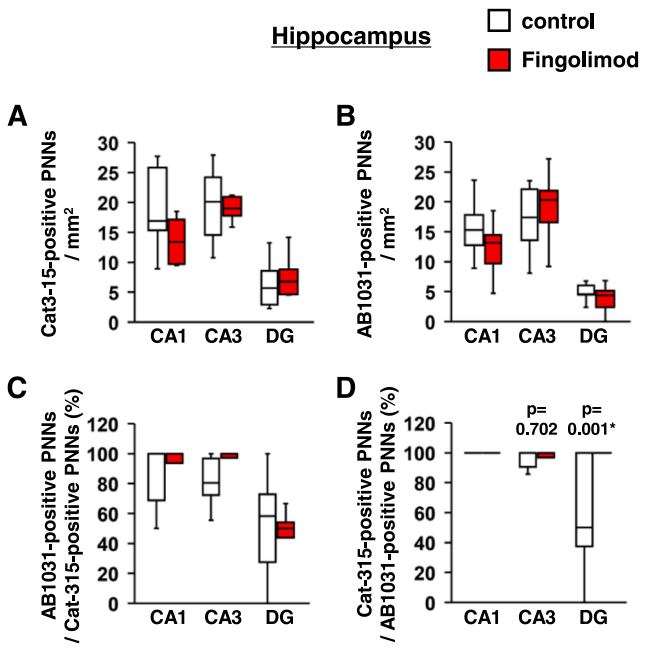

Fig. 10. Quantitative analyses of Cat-315-positive PNNs and AB1031-positive PNNs in the hippocampus of fingolimod-treated mice, Region-specific patterns of Cat-315-positive PNN density (A) and AB1031-positive PNN density (B) in the hippocampus. The percentages of Cat-315-positive PNNs containing AB1031 (C) and AB1031-positive PNNs containing Cat-315 (D) in the hippocampus are shown. Data are expressed as box plots (n = 10 mice/group). P-values were calculated using two-way ANOVA. *p < 0.05 for comparison of the same regions between fingolimod-treated groups.

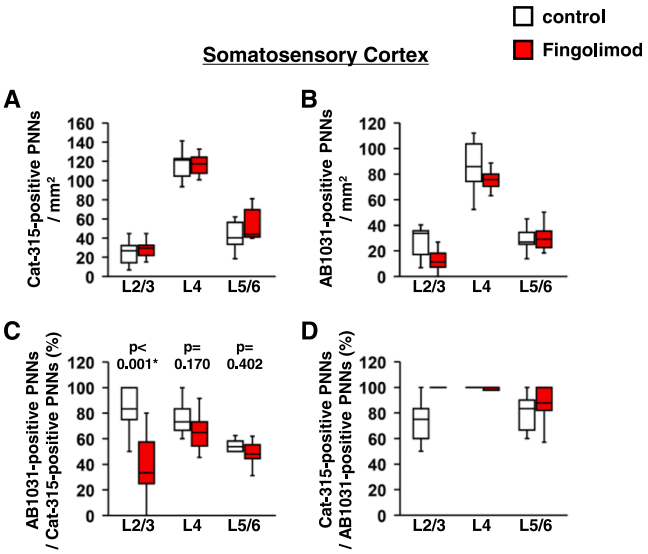

Fig. 11. Quantitative analyses of Cat-315-positive PNNs and AB1031-positive PNNs in the somatosensory cortex of fingolimod-treated mice, Layer-specific patterns of Cat-315-positive PNN density (A) and AB1031-positive PNN density (B) in the somatosensory cortex. The percentages of Cat-315-positive PNNs containing AB1031 (C) and AB1031-positive PNNs containing Cat-315 (D) in the somatosensory cortex are shown. Data are expressed as box plots (n = 10 mice/group). P-values were calculated using two-way ANOVA. *p < 0.05 for comparison of the same layers between the fingolimod-treated groups.

PV-positive neurons are a type of GABAergic inhibitory interneuron. It was necessary to confirm the effects of fingolimod, if any, on GABAergic inhibitory interneurons. GAD67 is a rate-determining enzyme responsible for more than 90% of GABA production (Asada et al., 1997). An increase in GAD67-positive neurons was observed in the hippocampus but not in the prefrontal and somatosensory cortices of the fingolimod-treated mice. Anti-GAD67 antibodies are used to label GABAergic neurons; however, not all GABAergic neurons can be labeled (Fujihara et al., 2015). Therefore, there are inhibitory neurons that

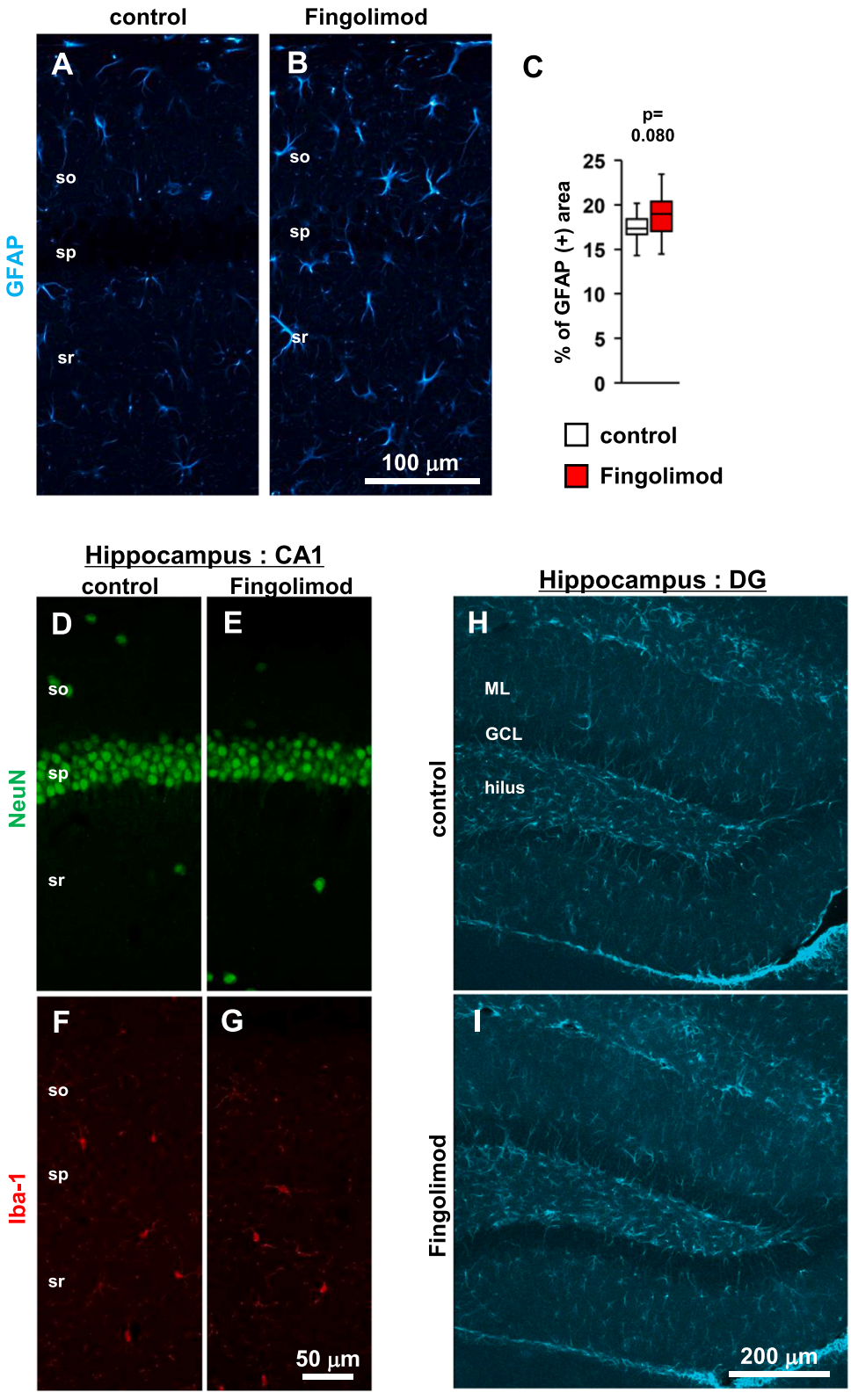

Fig. 12. GFAP-positive astrocytes, NeuN-positive cells, and Iba-1-positive microglia in the hippocampus of Fingolimod-treated mice, Representative immunofluorescent images showing the distribution of GFAP-positive astrocytes (A, B) in the CA1 of control (A) and fingolimod-treated mice (B). Percentage of GFAP-positive area in the CA1 of the hippocampus (C). Double confocal images of NeuN (D, E), and Iba-1 (F, G) in the CA1 of control (D, F) and fingolimod-treated mice (E, G). Representative immunofluorescent images showing the distribution of GFAP-positive cells in the DG of control (H) and fingolimod-treated mice (I). Scale bar = 100 μm in B (applies to A, B), 50 μm in G (applies to D, E, F, G), and 100 μm in I (applies to F, I). Data are expressed as box plots (n = 10 mice per group). P-values were calculated using Student's t-test. *$p < 0.05$ for comparison of the same regions between fingolimod-treated groups.

express PV, but have low expression levels of GAD67. Similarly, decreased GAD67 expression has been observed in various models of schizophrenia, including NMDA receptor dysfunction and dopamine sensitization models (Behrens et al., 2007; Lee et al., 2013). It is also possible that the administration of fingolimod increased the number of inhibitory interneurons that express PV but are low in GAD67. Further research is needed to clarify whether the increase in PV neurons observed in this study is due to an increase in inhibitory neurons or an increase in excitatory neurons expressing PV.

The therapeutic effects of fingolimod on the brain are mostly mediated by S1P1 (sphingosine-1-phosphate receptor 1) receptors, which are highly expressed in astrocytes and comparatively less expressed in

neurons, oligodendrocytes, and microglia (Choi et al., 2011). The protective effect of fingolimod has been reported to be greater in astrocytes than in microglia (Camós-Carreras et al., 2020). When astrocytes are activated, they become hypertrophied occupying more area (Borges et al., 2003; Shapiro et al., 2008). Fingolimod is a Food and Drug Administration approved drug for the remission of recurrent multiple sclerosis, which acts by reducing the activation of astrocytes (Brunkhorst et al., 2014). However, chronic administration of fingolimod did not increase the area occupied by astrocytes in the hippocampus of the mice indicating inactive astrocytes. Moreover, this may be due to differences in the fingolimod administration period, concentration, mouse strain, etc. Detailed studies are needed to clarify these differences.

We identified GFAP-positive neurons in DG with fingolimod treatment. In addition to astrocytes, GFAP is also expressed in neural stem cells involved in adult neurogenesis in the hippocampal DG (Song et al., 2002). When neurogenesis is inhibited, the number of GFAP-positive cells in DG decreases (Lazarov et al., 2010). In this study, chronic administration of fingolimod did not affect GFAP-positive cells.

Expression of PV proteins in PV-positive neurons is essential for cognitive function (Murray et al., 2011; Miyamae et al., 2017). When oxidative stress is generated in the mouse brain by drug administration, the number of PV neurons decreases (Behrens et al., 2007, 2008). PV neurons play an important role in regulating the firing of pyramidal cells. Abnormalities in PV-positive neurons have been reported in patients with schizophrenia and autism (Nahar et al., 2021; Lewis, 2012; Filice, 2020). This study indicates that the role of fingolimod in these diseases may be worth investigating in future studies.

Epidemiological data clearly emphasize that women are more likely to develop multiple sclerosis than men (Harbo et al., 2013). Human studies have also shown gender dependent variation of effects of fingolimod treatment (Manni et al., 2017). In this study, we used male mice whereas use of female mice might have a different outcome.

Conclusion

Chronic administration of fingolimod increased the density of PV-positive neurons in the hippocampus, prefrontal cortex, and somatosensory cortex. The results of this study indicate that fingolimod may be applied not only to the treatment of multiple sclerosis, but also to neuropsychiatric disorders related to PV-positive neurons.

Funding sources

This research did not receive any specific grants from funding agencies in the public commercial or not-for-profit sectors.

Data Availability

The datasets used and/or analyzed during the current study are available from the corresponding authors upon reasonable request.

Acknowledgements

We thank R. Kuyama and R. Fujita for technical assistance and the Kawasaki Medical School Central Research Institute for providing the instruments used in this study. We would also like to thank Editage (www.editage.jp) for their English language editing services.

Author Contributions

All authors had full access to all study data and take full responsibility for the integrity of the data and the accuracy of the data analysis. Study concept and design: H.U., M.O., and T.I.; Acquisition of data: H.U. and Y.T.; Analysis and interpretation of data: H.U. and Y.T.; Drafting of the manuscript: H.U. and M.O.; Critical revision of the manuscript for important intellectual content: S.M., K.W., Y.T., Y.M., and T.I.; Statistical analysis: H.U. and Y.T.; Study supervision: M.O. and T.I.

Conflict Of Interest

The authors declare they have no competing financial interests.

References

Alpár, A., Gärtner, U., Härtig, W., Brückner, G., 2006. Distribution of pyramidal cells associated with perineuronal nets in the neocortex of rat. Brain Res 1120, 13–22.
Asada, H., Kawamura, Y., Maruyama, K., Kume, H., Ding, R.G., Kanbara, N., Kuzume, H., Sanbo, M., Yagi, T., Obata, K., 1997. Cleft palate and decreased brain gamma-aminobutyric acid in mice lacking the 67-kDa isoform of glutamic acid decarboxylase. Proc. Natl. Acad. Sci. USA 94, 6496–6499.
Begum, M.R., Sng, J.C.G., 2017. Molecular mechanisms of experience-dependent maturation in cortical GABAergic inhibition. J. Neurochem 142, 649–661.
Behrens, M.M., Ali, S.S., Dao, D.N., Lucero, J., Shekhtman, G., Quick, K.L., Dugan, L.L., 2007. Ketamine-induced loss of phenotype of fast-spiking interneurons is mediated by NADPH-oxidase. Science 318, 1645–1647.
Behrens, M.M., Ali, S.S., Dugan, L.L., 2008. Interleukin-6 mediates the increase in NADPH-oxidase in the ketamine model of schizophrenia. J. Neurosci. 28, 13957–13966.
Björkholm, C., Monteggia, L.M., 2016. BDNF - a key transducer of antidepressant effects. Neuropharmacology 102, 72–79.
Blaho, V.A., Hla, T., 2014. An update on the biology of sphingosine 1-phosphate receptors. J. Lipid Res 55, 1596–1608.
Borges, K., Gearing, M., McDermott, D.L., Smith, A.B., Almonte, A.G., Wainer, B.H., Dingledine, R., 2003. Neuronal and glial pathological changes during epileptogenesis in the mouse pilocarpine model. Exp. Neurol. 182, 21–34.
Brinkmann, V., Billich, A., Baumruker, T., Heining, P., Schmouder, R., Francis, G., Aradhye, S., Burtin, P., 2010. Fingolimod (FTY720): discovery and development of an oral drug to treat multiple sclerosis. Nat. Rev. Drug Disco 9 (11), 883–897.
Brückner, G., Grosche, J., Schmidt, S., Härtig, W., Margolis, R.U., Delpech, B., Seidenbecher, C.I., Czaniera, R., Schachner, M., 2000. Postnatal development of perineuronal nets in wild-type mice and in a mutant deficient in tenascin-R. J. Comp. Neurol. 428, 616–629.
Brückner, G., Grosche, J., Hartlage-Rübsamen, M., Schmidt, S., Schachner, M., 2003. Region and lamina-specific distribution of extracellular matrix proteoglycans, hyaluronan and tenascin-R in the mouse hippocampal formation. J. Chem. Neuroanat. 26, 37–50.
Brunkhorst, R., Vutukuri, R., Pfeilschifter, W., 2014. Fingolimod for the treatment of neurological diseases-state of play and future perspectives. Front Cell Neurosci. 8, 283.
Caballero, A., Diah, K.C., Tseng, K.Y., 2013. Region-specific upregulation of parvalbumin-, but not calretinin-positive cells in the ventral hippocampus during adolescence. Hippocampus 23, 1331–1336.
Caillard, O., Moreno, H., Schwaller, B., Llano, I., Celio, M.R., Marty, A., 2000. Role of the calcium-binding protein parvalbumin in short-term synaptic plasticity. Proc. Natl. Acad. Sci. USA 97, 13372–13377.
Camós-Carreras, A., Alba-Arbalat, S., Dotti-Boada, M., Parrado-Carrillo, A., Bernal-Morales, C., Saiz, A., Sánchez-Dalmau, B., 2020. Late Onset Macular Oedema in a Patient with Multiple Sclerosis Treated with Fingolimod. Neuroophthalmology 45, 61–64.
Canto, C.B., Wouterlood, F.G., Witter, M.P., 2008. What does the anatomical organization of the entorhinal cortex tell us? Neural Plast. 2008, 381243.
Carulli, D., Pizzorusso, T., Kwok, J.C., Putignano, E., Poli, A., Forostyak, S., Andrews, M. R., Deepa, S.S., Glant, T.T., Fawcett, J.W., 2010. Animals lacking link protein have attenuated perineuronal nets and persistent plasticity. Brain 133, 2331–2347.
Chapman, C.A., Jones, R.S., Jung, M., 2008. Neuronal plasticity in the entorhinal cortex. Neural Plast. 2008, 314785.
Choi, J.W., Gardell, S.E., Herr, D.R., Rivera, R., Lee, C.W., Noguchi, K., Teo, S.T., Yung, Y.C., Lu, M., Kennedy, G., Chun, J., 2011. FTY720 (fingolimod) efficacy in an animal model of multiple sclerosis requires astrocyte sphingosine 1-phosphate receptor 1 (S1P1) modulation. Proc. Natl. Acad. Sci. USA 108, 751–756.
Deepa, S.S., Carulli, D., Galtrey, C., Rhodes, K., Fukuda, J., Mikami, T., Sugahara, K., Fawcett, J.W., 2006. Composition of perineuronal net extracellular matrix in rat brain: a different disaccharide composition for the net-associated proteoglycans. J. Biol. Chem. 281, 17789–17800.
Deogracias, R., Yazdani, M., Dekkers, M.P., Guy, J., Ionescu, M.C., Vogt, K.E., Barde, Y. A., 2012. Fingolimod, a sphingosine-1 phosphate receptor modulator, increases BDNF levels and improves symptoms of a mouse model of Rett syndrome. Proc. Natl. Acad. Sci. USA 109, 14230–14235.
Dino, M.R., Harroch, S., Hockfield, S., Matthews, R.T., 2006. Monoclonal antibody Cat-315 detects a glycoform of receptor protein tyrosine phosphatase beta/phosphacan early in CNS development that localizes to extrasynaptic sites prior to synapse formation. Neuroscience 142, 1055–1069.
Dityatev, A., Brückner, G., Dityateva, G., Grosche, J., Kleene, R., Schachner, M., 2007. Activity-dependent formation and functions of chondroitin sulfate-rich extracellular matrix of perineuronal nets. Dev. Neurobiol. 67, 570–588.
Donato, F., Rompani, S.B., Caroni, P., 2013. Parvalbumin-expressing basket-cell network plasticity induced by experience regulates adult learning. Nature 504, 272–276.

Efstathopoulos, P., Kourgiantaki, A., Karali, K., Sidiropoulou, K., Margioris, A.N., Gravanis, A., Charalampopoulos, I., 2015. Fingolimod induces neurogenesis in adult mouse hippocampus and improves contextual fear memory. Transl. Psychiatry 5 (11), e685.
Fagiolini, M., Jensen, C.L., Champagne, F.A., 2009. Epigenetic influences on brain development and plasticity. Curr. Opin. Neurobiol. 19, 207–212.
Favuzzi, E., Marques-Smith, A., Deogracias, R., Winterflood, C.M., Sánchez-Aguilera, A., Mantoan, L., Maeso, P., Fernandes, C., Ewers, H., Rico, B., 2017. Activity-Dependent Gating of Parvalbumin Interneuron Function by the Perineuronal Net Protein Brevican. Neuron 95, 639–655.
Filice, F., Janickova, L., Henzi, T., Bilella, A., Schwaller, B., 2020. The Parvalbumin Hypothesis of Autism Spectrum Disorder. Front Cell Neurosci. 14, 577525.
Fujihara, K., Miwa, H., Kakizaki, T., Kaneko, R., Mikuni, M., Tanahira, C., Tamamaki, N., Yanagawa, Y., 2015. Glutamate Decarboxylase 67 Deficiency in a Subset of GABAergic Neurons Induces Schizophrenia-Related Phenotypes. Neuropsychopharmacology 40, 2475–2486.
Fukumoto, K., Mizoguchi, H., Takeuchi, H., Horiuchi, H., Kawanokuchi, J., Jin, S., Mizuno, T., Suzumura, A., 2014. Fingolimod increases brain-derived neurotrophic factor levels and ameliorates amyloid β-induced memory impairment. Behav. Brain Res 268, 88–93.
Harbo, H.F., Gold, R., Tintoré, M., 2013. Sex and gender issues in multiple sclerosis. Ther. Adv. Neurol. Disord. 6, 237–248.
Hockfield, S., Sur, M., 1990. Monoclonal antibody Cat-301 identifies Y-cells in the dorsal lateral geniculate nucleus of the cat. J. Comp. Neurol. 300, 320–330.
Horii-Hayashi, N., Sasagawa, T., Matsunaga, W., Nishi, M., 2015. Development and Structural Variety of the Chondroitin Sulfate Proteoglycans-Contained Extracellular Matrix in the Mouse Brain. Neural Plast. 2015, 256389.
Huang, Z.J., Kirkwood, A., Pizzorusso, T., Porciatti, V., Morales, B., Bear, M.F., Maffei, L., Tonegawa, S., 1999. BDNF regulates the maturation of inhibition and the critical period of plasticity in mouse visual cortex. Cell 98, 739–755.
Jeanmonod, D., Rice, F.L., Van der Loos, H., 1981. Mouse somatosensory cortex: alterations in the barrelfield following receptor injury at different early postnatal ages. Neuroscience 6, 1503–1535.
Jung, M.W., Baeg, E.H., Kim, M.J., Kim, Y.B., Kim, J.J., 2008. Plasticity and memory in the prefrontal cortex. Rev. Neurosci. 19, 29–46.
Kolb, B., Gibb, R., 2015. Plasticity in the prefrontal cortex of adult rats. Front Cell Neurosci. 9, 15.
Kolb, B., Harker, A., Gibb, R., 2017. Principles of plasticity in the developing brain. Dev. Med Child Neurol. 59, 1218–1223.
Lazarov, O., Mattson, M.P., Peterson, D.A., Pimplikar, S.W., van Praag, H., 2010. When neurogenesis encounters aging and disease. Trends Neurosci. 33, 569-79.
Lee, F.H., Zai, C.C., Cordes, S.P., Roder, J.C., Wong, A.H., 2013. Abnormal interneuron development in disrupted-in-schizophrenia-1 L100P mutant mice. Mol. Brain 6, 20.
Lewis, D.A., 2012. Cortical circuit dysfunction and cognitive deficits in schizophrenia–implications for preemptive interventions. Eur. J. Neurosci. 35, 1871–1878.
Maeda, N., 2015. Proteoglycans and neuronal migration in the cerebral cortex during development and disease. Front. Neurosci. 9, 98.
Maffei, A., Nataraj, K., Nelson, S.B., Turrigiano, G.G., 2006. Potentiation of cortical inhibition by visual deprivation. Nature 443, 81–84.
Malberg, J.E., Eisch, A.J., Nestler, E.J., Duman, R.S., 2000. Chronic antidepressant treatment increases neurogenesis in adult rat hippocampus. J. Neurosci. 20, 9104–9110.
Manni, A., Direnzo, V., Iaffaldano, A., Di Lecce, V., Tortorella, C., Zoccolella, S., Iaffaldano, P., Trojano, M., Paolicelli, D., 2017. Gender differences in safety issues during Fingolimod therapy: Evidence from a real-life Relapsing Multiple Sclerosis cohort. Brain Behav. 7 (10), e00804.
McRae, P.A., Rocco, M.M., Kelly, G., Brumberg, J.C., Matthews, R.T., 2007. Sensory deprivation alters aggrecan and perineuronal net expression in the mouse barrel cortex. J. Neurosci. 27, 5405–5413.
Miyamae, T., Chen, K., Lewis, D.A., Gonzalez-Burgos, G., 2017. Distinct Physiological Maturation of Parvalbumin-Positive Neuron Subtypes in Mouse Prefrontal Cortex. J. Neurosci. 37, 4883–4902.
Murray, A.J., Sauer, J.F., Riedel, G., McClure, C., Ansel, L., Cheyne, L., Bartos, M., Wisden, W., Wulff, P., 2011. Parvalbumin-positive CA1 interneurons are required for spatial working but not for reference memory. Nat. Neurosci. 14, 297–299.
Nabel, E.M., Morishita, H., 2013. Regulating critical period plasticity: insight from the visual system to fear circuitry for therapeutic interventions. Front Psychiatry 4, 146.
Nahar, L., Delacroix, B.M., Nam, H.W., 2021. The Role of Parvalbumin Interneurons in Neurotransmitter Balance and Neurological Disease. Front Psychiatry 12, 679960.
Nakamura, M., Nakano, K., Morita, S., Nakashima, T., Oohira, A., Miyata, S., 2009. Expression of chondroitin sulfate proteoglycans in barrel field of mouse and rat somatosensory cortex. Brain Res 1252, 117–129.
di Nuzzo, L., Orlando, R., Tognoli, C., Di Pietro, P., Bertini, G., Miele, J., Bucci, D., Motolese, M., Scaccianoce, S., Caruso, A., Mauro, G., De Lucia, C., Battaglia, G., Bruno, V., Fabene, P.F., Nicoletti, F., 2015. Antidepressant activity of fingolimod in mice. Pharm. Res Perspect. 3 (3), e00135.
Paxinos, G., Franklin, K.B.J.Paxinos, 2013. and Franklin's the mouse brain in stereotaxic coordinates, 4th ed..,. Academic Press,.
Rowlands, D., Lensjø, K.K., Dinh, T., Yang, S., Andrews, M.R., Hafting, T., Fyhn, M., Fawcett, J.W., Dick, G., 2018. Aggrecan Directs Extracellular Matrix-Mediated Neuronal Plasticity. J. Neurosci. 38, 10102–10113.
Saarelainen, T., Hendolin, P., Lucas, G., Koponen, E., Sairanen, M., MacDonald, E., Agerman, K., Haapasalo, A., Nawa, H., Aloyz, R., Ernfors, P., Castrén, E., 2003. Activation of the TrkB neurotrophin receptor is induced by antidepressant drugs and is required for antidepressant-induced behavioral effects. J. Neurosci. 23, 349–357.
Sadato, N., Yamada, H., Okada, T., Yoshida, M., Hasegawa, T., Matsuki, K., Yonekura, Y., Itoh, H., 2004. Age-dependent plasticity in the superior temporal sulcus in deaf humans: a functional MRI study. BMC Neurosci. 5, 56.
Santarelli, L., Saxe, M., Gross, C., Surget, A., Battaglia, F., Dulawa, S., Weisstaub, N., Lee, J., Duman, R., Arancio, O., Belzung, C., Hen, R., 2003. Requirement of hippocampal neurogenesis for the behavioral effects of antidepressants. Science 301, 805–809.
Schmalbach, B., Lepsveridze, E., Djogo, N., Papashvili, G., Kuang, F., Leshchyns'ka, I., Sytnyk, V., Nikonenko, A.G., Dityatev, A., Jakovcevski, I., Schachner, M., 2015. Age-dependent loss of parvalbumin-expressing hippocampal interneurons in mice deficient in CHL1, a mental retardation and schizophrenia susceptibility gene. J. Neurochem 135, 830–844.
Senn, C., Kutsche, M., Saghatelyan, A., Bösl, M.R., Löhler, J., Bartsch, U., Morellini, F., Schachner, M., 2002. Mice deficient for the HNK-1 sulfotransferase show alterations in synaptic efficacy and spatial learning and memory. Mol. Cell Neurosci. 20, 712–729.
Shapiro, L.A., Wang, L., Ribak, C.E., 2008. Rapid astrocyte and microglial activation following pilocarpine-induced seizures in rats. Epilepsia 49 (Suppl 2), 33–41.
Slaker, M., Blacktop, J.M., Sorg, B.A., 2016. Caught in the Net: Perineuronal Nets and Addiction. Neural Plast. 2016, 7538208.
Smith, G.B., Bear, M.F., 2010. Bidirectional ocular dominance plasticity of inhibitory networks: recent advances and unresolved questions. Front Cell Neurosci. 4, 21.
Sohal, V.S., Zhang, F., Yizhar, O., Deisseroth, K., 2009. Parvalbumin neurons and gamma rhythms enhance cortical circuit performance. Nature 459, 698–702.
Song, H., Stevens, C.F., Gage, F.H., 2002. Astroglia induce neurogenesis from adult neural stem cells. Nature 417, 39–44.
Sun, Y., Nguyen, A.Q., Nguyen, J.P., Le, L., Saur, D., Choi, J., Callaway, E.M., Xu, X., 2014. Cell-type-specific circuit connectivity of hippocampal CA1 revealed through Cre-dependent rabies tracing. Cell Rep. 7, 269–280.
Sur, M., 1988. Development and plasticity of retinal X and Y axon terminations in the cat's lateral geniculate nucleus. Brain Behav. Evol. 31, 243–251.
Tyler, W.J., Alonso, M., Bramham, C.R., Pozzo-Miller, L.D., 2002. From acquisition to consolidation: on the role of brain-derived neurotrophic factor signaling in hippocampal-dependent learning. Learn Mem. 9, 224–237.
Ueno, H., Suemitsu, S., Okamoto, M., Matsumoto, Y., Ishihara, T., 2017. Parvalbumin neurons and perineuronal nets in the mouse prefrontal cortex. Neuroscience 343, 115–127.
Ueno, H., Suemitsu, S., Okamoto, M., Matsumoto, Y., Ishihara, T., 2017. Sensory experience-dependent formation of perineuronal nets and expression of Cat-315 immunoreactive components in the mouse somatosensory cortex. Neuroscience 355, 161–174.
Ueno, H., Suemitsu, S., Murakami, S., Kitamura, N., Wani, K., Okamoto, M., Aoki, S., Ishihara, T., 2017. Postnatal development of GABAergic interneurons and perineuronal nets in mouse temporal cortex subregions. Int J. Dev. Neurosci. 63, 27–37.
Ueno, H., Takao, K., Suemitsu, S., Murakami, S., Kitamura, N., Wani, K., Okamoto, M., Aoki, S., Ishihara, T., 2018. Age-dependent and region-specific alteration of parvalbumin neurons and perineuronal nets in the mouse cerebral cortex. Neurochem Int 112, 59–70.
Vidal-Martínez, G., Vargas-Medrano, J., Gil-Tommee, C., Medina, D., Garza, N.T., Yang, B., Segura-Ulate, I., Dominguez, S.J., Perez, R.G., 2016. FTY720/Fingolimod Reduces Synucleinopathy and Improves Gut Motility in A53T Mice: CONTRIBUTIONS OF PRO-BRAIN-DERIVED NEUROTROPHIC FACTOR (PRO-BDNF) AND MATURE BDNF. J. Biol. Chem. 291, 20811–20821.
Yazaki-Sugiyama, Y., Kang, S., Cãteau, H., Fukai, T., Hensch, T.K., 2009. Bidirectional plasticity in fast-spiking GABA circuits by visual experience. Nature 462, 218–221.
Ye, Q., Miao, Q.L., 2013. Experience-dependent development of perineuronal nets and chondroitin sulfate proteoglycan receptors in mouse visual cortex. Matrix Biol. 32, 352–363.